Dynamics of a qubit coupled to a broadened harmonic mode at finite detuning

2007 New J. Phys. 9 316

(http://iopscience.iop.org/1367-2630/9/9/316)

New Journal of Physics
The open–access journal for physics

Dynamics of a qubit coupled to a broadened harmonic mode at finite detuning

F Nesi[1], **M Grifoni**[1] **and E Paladino**[2]

[1] Institut für Theoretische Physik, Universität Regensburg, 93035 Regensburg, Germany
[2] MATIS INFM-CNR and Dipartimento di Metodologie Fisiche e Chimiche, Università di Catania, 95125 Catania, Italy
E-mail: milena.grifoni@physik.uni-regensburg.de

New Journal of Physics **9** (2007) 316
Received 24 June 2007
Published 10 September 2007
Online at http://www.njp.org/
doi:10.1088/1367-2630/9/9/316

Abstract. We study the dynamics of a symmetric two-level system strongly coupled to a broadened harmonic mode. Upon mapping the problem on to a spin–boson model with peaked spectral density, we show how analytic solutions can be obtained, at arbitrary detuning and finite temperatures, in the case of large Q-factors of the oscillator. One, two or more dominating oscillation frequencies of the two-level particle can be observed as a consequence of the entanglement with the oscillator. Our approximated analytical solution agrees well with numerical predictions obtained within the non-interacting blip approximation.

PII: S1367-2630(07)53530-5

Contents

1. Introduction

A prominent physical model to study dissipative and decoherence effects in quantum mechanics is the spin–boson model [1]–[3]. Currently, we are witnessing its revival since it allows a quantitative description of solid-state quantum bits (qubits) [4]. A more realistic description requires the inclusion of external control fields as well as of a detector. In the spin–boson model, the environment is characterized by a spectral density $G(\omega)$. If the environment is formed by a quantum detector which itself is damped by Ohmic fluctuations, the form of the spectral density can become nontrivial, as it also reflects internal resonances of the detector. An example is provided by a flux-qubit read out by a dc-SQUID (superconducting quantum interference device) [5]–[7] which gives rise to an effective spectral density $G_{\rm eff}(\omega)$ for the qubit with a peak at the dc-SQUID plasma frequency Ω [8, 9] of width Γ, cf equation (2) below. As shown in [10] under general grounds, such a spin–boson Hamiltonian can be exactly mapped on to that of a two-state-system (TSS) coupled to a single harmonic oscillator (HO) mode of frequency Ω with coupling strength g. The HO itself interacts with a set of harmonic oscillators with spectral density of the continuous bath modes $G_{\rm Ohm}(\omega) = \kappa\omega$. The mapping between the two models is completed with $\Gamma = 2\pi\kappa\Omega$ and $\alpha = \lim_{\omega\to 0} G_{\rm eff}(\omega)/2\omega = 8\kappa g^2/\Omega^2$. Thus, besides the case of a damped dc-SQUID inductively coupled to a flux qubit, the spin–boson model with peaked spectral density $G_{\rm eff}$ can describe the generic situation of a two-level-particle coupled to a damped harmonic mode. This is realized e.g. in atom-based cavity quantum electrodynamics [11], circuit quantum electrodynamics with superconducting systems [12, 13], semiconducting quantum dots in nanocavities [14] and in nanomechanical resonators [15]. In particular, in the seminal experiment [12] the vacuum Rabi splitting was demonstrated in a Cooper-pair-box resonantly coupled to a cavity mode (i.e. for $\delta \ll g$, where the detuning δ is the difference between the HO frequency Ω and the TSS transition frequency). Recently, in the same system Schuster *et al* [13] demonstrated, in the dispersive regime $\delta > g$, the so-called 'number splitting', i.e. the qubit dephasing spectrum was used to probe the photon number distribution.

From the theoretical point of view, a large amount of literature exists, in which a coupled TSS–HO is considered as the central quantum system, and the effects of the Ohmic bath are treated perturbatively. However, in these works one usually does not solve the original coupled TSS–HO Hamiltonian, but rather approximated forms to it expected to be valid e.g. in the resonant regime ($\delta \ll g$) [11, 16], or in the dispersive regime (large detuning $\delta \gg g$) [17]–[21]. Specifically, for the case e.g. of circuit QED (at the charge degeneracy point), a rotating wave approximation (RWA) expected to be valid for small detuning yields the Jaynes–Cummings Hamiltonian [22]. On the other hand, in the dispersive regime neglecting terms of order δ^2/g^2 yields the quantum version of the ac-Stark Hamiltonian [16, 17]. Recently, exact real-time path-integral calculations have been performed [23], based on the numerical QUAPI (quasiadiabatic propagator path-integral) method, covering the resonant, as well as the dispersive regime, and testing the reliability of the RWA in the resonant regime. The case of a (damped) TSS–HO dynamics was treated beyond the RWA in [24, 25], upon truncation of the number of relevant states of the central TSS–HO system.

An alternative, equivalent, point of view, is the spin–boson model with peaked spectrum. The advantage of this approach is that the reduced density matrix has rank 2. Moreover, no RWA approximations are required to reduce the problem to simpler effective Hamiltonians. The peculiar feature of the peaked spectrum (2) is reflected in the form of the bath correlation functions, cf (4a) and (4b) below. Until now, the effects of such a structured spectral density on the decoherence properties of a qubit have been studied in [26]–[28] within a perturbative approach in $G_{\rm eff}$. It was shown in [23] that such a perturbative scheme breaks down for strong qubit-detector coupling $g \gg \Gamma$, and when the qubit and detector frequencies are comparable. Hence, nonperturbative schemes, as the *ab-initio* QUAPI [23], the non-interacting blip approximation (NIBA) [28], the flow-equation method [28, 29] or a generalized polaron transformation [30] have been used. However, a closed form analytic expression for the qubit population has not been provided so far.

In this work, we show how to investigate the dynamics of a spin–boson system with a structured environment, in the case of a strong coupling between qubit and oscillator and for small detector–bath coupling strength, $\kappa = \Gamma/2\pi\Omega \ll 1$, corresponding to large quality factors of the oscillator. We evaluate the dynamics upon starting from the (nonperturbative in $G_{\rm eff}$) non-interacting blip approximation (NIBA) [1, 2]. Analytical results, valid also at *arbitrary* detuning, are obtained by approximating the NIBA kernels up to first-order in the detector–bath coupling strength κ. It is shown that the coupling to the damped oscillator yields the possibility of a multiple-peaks structure of the TSS spectrum. The position and height of the peaks depend in a nontrivial way on the temperature, as well as on the TSS coupling strength g. In particular, in the regime $\Gamma \ll g \ll \Omega$ and $k_{\rm B}T < \hbar\Omega$ only two oscillation frequencies dominate the spectrum. Notice that this result encompasses the coherent splitting also obtained in the Jaynes–Cumming approximation, as well as the number splitting effect discussed for the dispersive regime [13, 21], as our theory holds true for arbitrary detuning as long as the Q-factor of the oscillator is large.

The paper is organized as follows: in the next section, we will introduce the model. Then in section 3, we discuss the well-known and widely used NIBA and its predictions. Analytical results for the dynamics are derived in section 4. Conclusions are drawn in section 5.

2. The model

Let us consider the spin–boson Hamiltonian describing the interaction of a symmetric TSS with a structured environment. It reads [1, 2]

$$H_{\rm SB}(t) = -\frac{\hbar\Delta}{2}\sigma_x + \frac{1}{2}\sigma_z\hbar\sum_k \tilde{\lambda}_k(\tilde{b}_k^\dagger + \tilde{b}_k) + \sum_k \hbar\tilde{\omega}_k\tilde{b}_k^\dagger\tilde{b}_k, \tag{1}$$

where σ_i are Pauli matrices and $\hbar\Delta$ is the tunnel splitting. Moreover, $\tilde{b}_k$ is the annihilation operator of the kth bath mode with frequency $\tilde{\omega}_k$. In the spin–boson model, the influence of the environment is fully characterized by a so-called spectral function, which we assume to be of the form

$$G_{\rm eff}(\omega) = \sum_k \tilde{\lambda}_k^2\delta(\omega - \tilde{\omega}_k) = \frac{2\alpha\omega\Omega^4}{(\Omega^2-\omega^2)^2 + (\Gamma\omega)^2}. \tag{2}$$

It has a Lorentzian peak of width Γ at the characteristic frequency Ω, and behaves ohmically at low frequencies with the dimensionless coupling strength $\alpha = \lim_{\omega\to 0} G_{\rm eff}(\omega)/2\omega$. Specifically, in the spin–boson model, the environmental effects are captured in the so-called bath correlation function

$$Q(\tau) \equiv Q'(\tau) + {\rm i}Q''(\tau) = \int_0^\infty {\rm d}\omega \frac{G_{\rm eff}(\omega)}{\omega^2}\left[\coth\left(\frac{\hbar\omega\beta}{2}\right)(1-\cos\omega t) + {\rm i}\sin\omega t\right], \tag{3}$$

which for the effective spectral density (2) takes the form [2]

$$Q'(\tau) = X\tau + L\left({\rm e}^{-(\Gamma/2)\tau}\cos\bar{\Omega}\tau - 1\right) + Z{\rm e}^{-(\Gamma/2)\tau}\sin\bar{\Omega}\tau + Q'_{\rm Mats}(\tau), \tag{4a}$$

$$Q''(\tau) = \pi\alpha - {\rm e}^{-(\Gamma/2)\tau}\pi\alpha\left(N\sin\bar{\Omega}\tau + \cos\bar{\Omega}\tau\right). \tag{4b}$$

The quantity $\bar{\Omega} = \sqrt{\Omega^2 - (\Gamma^2/4)}$ corresponds in the underdamped regime $\Gamma < \Omega$ to a renormalized oscillator frequency of the oscillator, while in the overdamped case $\Gamma > \Omega$ describes an exponential decay. The temperature dependent prefactors are

$$X = \frac{2\pi\alpha}{\hbar\beta}, \tag{5}$$

$$L = \frac{\pi\alpha}{\Gamma\bar{\Omega}}\frac{1}{\cosh(\beta\hbar\bar{\Omega}) - \cos(\beta(\hbar\Gamma/2))}\left[\left(\frac{\Gamma^2}{4} - \bar{\Omega}^2\right)\sinh(\beta\hbar\bar{\Omega}) + \Gamma\bar{\Omega}\sin(\beta(\hbar\Gamma/2))\right], \tag{6}$$

$$Z = \frac{\pi\alpha}{\Gamma\bar{\Omega}}\frac{1}{\cosh(\beta\hbar\bar{\Omega}) - \cos(\beta(\hbar\Gamma/2))}\left[-\Gamma\bar{\Omega}\sinh(\beta\hbar\bar{\Omega}) + \left(\frac{\Gamma^2}{4} - \bar{\Omega}^2\right)\sin(\beta(\hbar\Gamma/2))\right], \tag{7}$$

and $N = \frac{1}{\Gamma\bar{\Omega}}(\Gamma^2/4 - \bar{\Omega}^2)$. Finally, $Q'_{\rm Mats}(\tau)$ is a function of Matsubara frequencies $\nu_n \equiv (2\pi/h\beta)n$, and it has the form

$$Q'_{\rm Mats}(\tau) = -4\pi\alpha\frac{\Omega^4}{\hbar\beta}\sum_{n=1}^{+\infty}\frac{1}{(\Omega^2+\nu_n^2)^2 - \Gamma^2\nu_n^2}\left[\frac{{\rm e}^{-\nu_n\tau}-1}{\nu_n}\right]. \tag{8}$$

For temperatures $k_{\rm B}T > (\hbar\Gamma/2\pi)$, contributions coming from the Matsubara term can be neglected [2][3], as done in the rest of this work. We notice that since we are interested in the

[3] In the low temperature regime $k_{\rm B}T \ll (\hbar\Gamma/2\pi)$ the bath-correlation function decays on a timescale set by the first Matsubara frequency ν_1.

large Q-factors limit, i.e. $\Gamma/2\pi\Omega \ll 1$, this constraint still allows investigation of the high temperature regime $k_{\rm B}T > \hbar\Omega$, as well as the low temperature regime $\hbar\Omega > k_{\rm B}T \gg \hbar\Gamma/2\pi$.

The qubit dynamics is described by the reduced density operator $\rho(t)$ obtained by tracing out the environmental degrees of freedom. We investigate the population difference $P(t) := \langle\sigma_z\rangle_t = {\rm Tr}\{\rho(t)\sigma_z\}$. Such a dynamical quantity $P(t)$ obeys the exact generalized master equation (GME) [2]

$$\dot{P}(t) = -\int_0^t {\rm d}t'\, K(t-t')P(t') \qquad t > 0, \tag{9}$$

with the kernels $K(t)$ being a series expression in the number of tunneling transitions. Since equation (9) involves only convolutions, it can be solved by using Laplace transforms. The GME yields as

$$P(\lambda) = \frac{1}{\lambda + K(\lambda)}, \tag{10}$$

where the same symbols $P(\lambda)$ and $K(\lambda)$ for the Laplace transform of $P(t)$ and $K(\tau)$ have been used, respectively. From equation (10), it follows that in order to obtain $P(t)$ one has to solve the pole equation

$$\lambda + K(\lambda) = 0, \tag{11}$$

and then inverse transform to the time space. Due to the intricate form of the exact kernel $K(t)$ (or $K(\lambda)$), equations (9) or (10) cannot be solved neither numerically nor analytically. We must therefore invoke some approximations. For the symmetric spin–boson model (1), the so-called NIBA discussed in the next section is expected to yield reliable results over the *whole* regime of parameters.

3. Non-interacting blip approximation (NIBA)

Within the NIBA [1, 2], of the exact series expression for $K(\lambda)$, only the first term of second-order in the tunneling frequency Δ is retained. This amounts to neglecting bath-induced inter-blip correlations, where the 'blips' denote time intervals spent in off-diagonal states of the TSS reduced density matrix [1]. This approximation has been commonly used over the whole range of temperatures and coupling strength to describe the dynamics of a symmetric spin–boson system. In the symmetric case in fact, terms linear in the (weak) inter-blip correlations vanish[4]. In the NIBA, the kernel has the very simple form

$$K(t) = \Delta^2 {\rm e}^{-Q'(t)} \cos\big(Q''(t)\big), \tag{12}$$

or in the Laplace space

$$K(\lambda) = \Delta^2 \int_0^\infty {\rm d}\tau\, {\rm e}^{-\lambda\tau} {\rm e}^{-Q'(\tau)} \cos\big(Q''(\tau)\big), \tag{13}$$

where the bath correlation functions $Q'(\tau)$ and $Q''(\tau)$ have been introduced in equation (4). Typical results for $P(t)$ obtained from the numerical integration of the NIBA master equation for the resonant case $\Omega = \Delta$ and at finite detuning $\Omega = 1.5\Delta$ are shown in figures 1 and 2,

[4] From inspection of (4a) it follows that the inter-blip correlations, being expressed as difference of four Q' functions [2], are long ranged but weak, as they are solely determined by the (bounded) decaying oscillatory parts of $Q'(t)$.

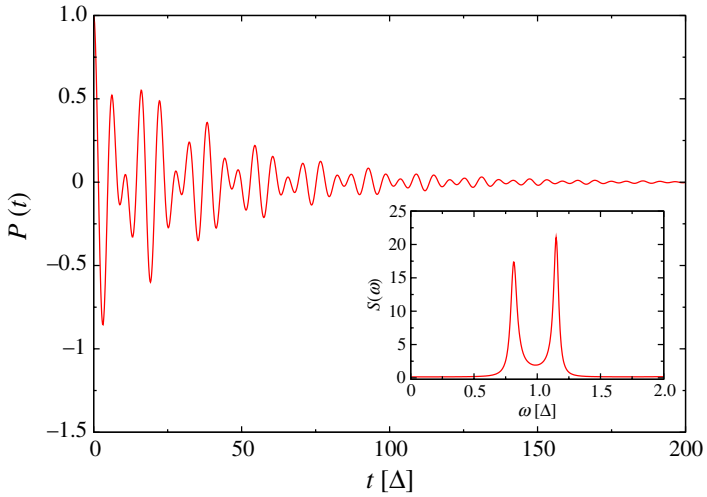

Figure 1. Time evolution of the population difference $P(t)$ of a symmetric TSS in the resonant case $\Omega = 1$. The parameters are: $\Gamma = 0.097$, $T = 0.1$ (all frequencies are expressed in units of Δ) and $\alpha = 4 \times 10^{-3}$ (yielding $g = 0.18$). In this range of parameters, one clearly sees that the dynamics is dominated by *two* frequencies. Inset: the Fourier transform $S(\omega)$ of $P(t)$ displays two peaks, centered symmetrically around Ω. The distance between the peaks is approximately $2g$.

respectively. In the resonant case $P(t)$ exhibits a very pronounced beating pattern. The analysis of the corresponding spectrum

$$S(\omega) \equiv 2 \int_0^\infty \mathrm{d}t \cos(\omega t)\, P(t), \tag{14}$$

for the parameters choice of figure 1 (resonant case) clearly reveals the presence of two frequencies, which lie around $\Omega_\pm \approx \Omega \pm g$, where g is the coupling strength in the TSS + HO model. This is in agreement with the expectations obtained from a Jaynes–Cummings model [22]. However, as shown in the next section, for our case of a thermalized oscillator, and beyond the RWA approximation, the dependence of TSS frequencies on temperature, as well as on the coupling parameter g and on the frequency Ω is nontrivial, cf equation (47). The Fourier spectrum for the detuned case in figure 2 shows a more pronounced oscillation frequency, the relative magnitude of the two peaks becoming larger when the detuning is increased. Finally, as one raises the coupling strength g between TSS and HO, multiple resonances appear, see figure 3. These beating patterns clearly originate from the peaked nature of the environmental spectrum and are thus absent in the more frequently investigated cases of unstructured environments [1, 2], i.e. $G(\omega) \propto \omega^s \mathrm{e}^{-\omega/\omega_c}$, $s > 0$. The nature of the beatings, as well as an analytical approximation to $P(t)$ are discussed in the following section. The starting point is equation (10) and its related pole equation (11).

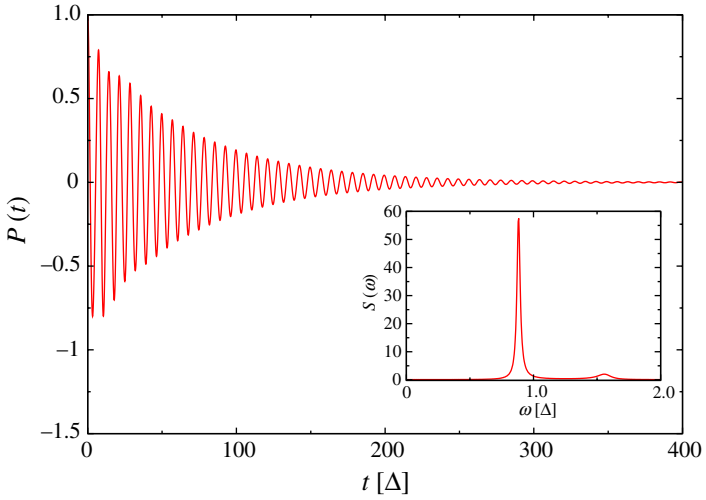

Figure 2. Time evolution of the population difference $P(t)$ of a symmetric TSS in the case of a finite detuning $\Omega = 1.5$. The parameters are: $\Gamma = 0.145$, $T = 0.1$ (all frequencies are expressed in units of Δ) and $\alpha = 5 \times 10^{-3}$ ($g = 0.3$). For this case of the TSS being off-resonance with the HO, one oscillation frequency dominates. Notice the relative magnitude of the two peaks of the Fourier transform shown in the inset.

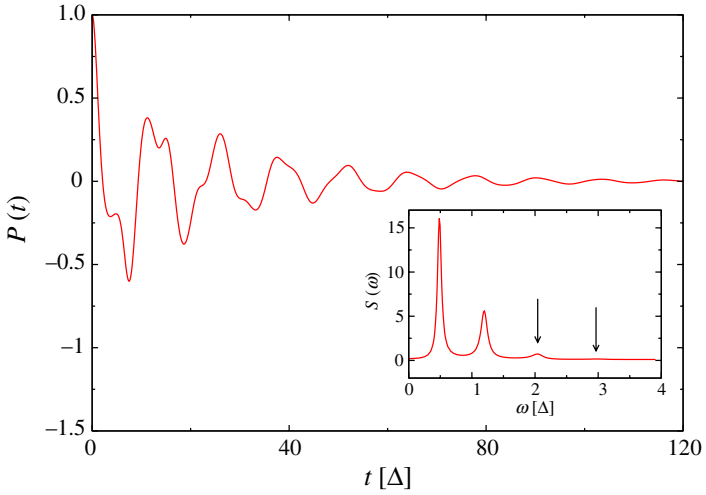

Figure 3. Time evolution of the population difference $P(t)$ of a symmetric TSS in the resonant case $\Omega = 1$. The parameters are: $\Gamma = 0.097$, $T = 0.1$ (all frequencies are expressed in units of Δ) as in figure 1, but now $\alpha = 3 \times 10^{-2}$ (yielding $g = 0.5$). In this range of parameters the dynamics is dominated by *four* frequencies. Inset: the Fourier transform $S(\omega)$ of $P(t)$ displays four peaks.

4. Weak-damping approximation (WDA) for a symmetric TSS

In the following, we shall derive an analytical expression for $P(t)$, based on the NIBA, valid for *arbitrary* detuning $|\Delta - \Omega| = \delta$. The key idea is that, since we are looking to a sharply peaked spectral density, i.e. $\kappa = \Gamma/2\pi\Omega \ll 1$, an expansion of the NIBA kernel (13) up to

first-order in κ is justified. Since the bath-correlation functions Q' and Q'' (equation (4b)) depend in a nontrivial way on κ, this requires some attention. In the end, we obtain

$$Q'(\tau) = \overbrace{Y\,(\cos\Omega\tau - 1)}^{Q_0'(\tau)} + \overbrace{A\tau\cos\Omega\tau + B\tau + C\sin\Omega\tau}^{Q_1'(\tau)} + \mathcal{O}[\kappa^2], \tag{15a}$$

$$Q''(\tau) = \underbrace{W\sin\Omega\tau}_{Q_0''(\tau)} + \underbrace{V\left(1 - \cos\Omega\tau - \frac{\Omega}{2}\tau\sin\Omega\tau\right)}_{Q_1''(\tau)} + \mathcal{O}[\kappa^2], \tag{15b}$$

with the zero-order terms

$$Y = -\frac{4g^2}{\Omega^2}\coth\frac{\beta\hbar\Omega}{2}, \qquad W = \frac{4g^2}{\Omega^2}, \tag{16}$$

and first-order terms

$$A = -\Gamma\frac{Y}{2}, \qquad B = \Gamma\frac{8g^2}{\Omega^3\hbar\beta}, \tag{17}$$

$$C = -\Gamma\frac{2g^2}{\Omega^3}\,\frac{\beta\hbar\Omega + 2\sinh\beta\hbar\Omega}{\cosh\beta\hbar\Omega - 1}, \qquad V = \Gamma\frac{4g^2}{\Omega^3}. \tag{18}$$

Notice that the contribution coming from the Matsubara frequencies (8) has been neglected. We will here discuss first the simpler undamped case ($\kappa = 0$) and later perform the WDA on the NIBA kernels.

4.1. Undamped case ($\kappa = 0$)

In this subsection, we discuss the case of a TSS coupled with an undamped HO initially prepared in a thermal equilibrium state. The pole equation now reads

$$\lambda_\mathrm{p} + K_0(\lambda_\mathrm{p}) = 0\,, \tag{19}$$

with

$$K_0(\lambda) = \Delta^2\int_0^\infty \mathrm{d}\tau\,\mathrm{e}^{-\lambda\tau}\,\mathrm{e}^{-Q_0'(\tau)}\cos\left(Q_0''(\tau)\right), \tag{20}$$

where we denoted with λ_p the solution of the undamped pole equation. Notice that $K_0(\lambda)$ has the same expression as in equation (13), if one replaces Q' and Q'' with Q_0' and Q_0'', respectively. In order to investigate equation (20), we replace $\cos(Q_0''(\tau))$ with $\mathrm{Re}\{\exp(\mathrm{i}Q_0''(\tau))\}$ and we perform the Jacobi–Anger expansion [31]

$$\mathrm{e}^{\mathrm{i}z\cos y} \equiv J_0(z) + 2\sum_{n=1}^{+\infty}\mathrm{i}^n J_n(z)\cos(ny), \tag{21}$$

where $J_n(z)$ are Bessel functions of a complex argument. We also make use of Graf's addition theorem

$$\sum_{k=-\infty}^{\infty} J_{n+k}(u)\,J_k(v)\begin{matrix}\cos\\ \sin\end{matrix}(k\alpha) = J_n(w)\begin{matrix}\cos\\ \sin\end{matrix}(n\chi), \tag{22}$$

where

$$w = \sqrt{u^2 + v^2 - 2\,u\,v\,\cos\alpha}, \tag{23}$$

and

$$\begin{cases} u - v\cos\alpha = w\cos\chi, & (24a) \\ v\sin\alpha = w\sin\chi. & (24b) \end{cases}$$

We finally obtain (see appendix A)

$$K_0(\lambda) = \Delta^2 \mathrm{e}^Y \int_0^\infty \mathrm{d}\tau \mathrm{e}^{-\lambda\tau} \mathrm{Re}\left[J_0(u_0) + 2\sum_{n=1}^{+\infty} \mathrm{i}^n J_n(u_0) \cos\left[n\left(\Omega t - \pi + \mathrm{i}\frac{\beta\hbar\Omega}{2} \right) \right] \right], \tag{25}$$

where

$$u_0 = \mathrm{i}\sqrt{Y^2 - W^2} = \mathrm{i}\frac{4g^2}{\Omega^2}\frac{1}{\sinh\left(\beta\hbar\Omega/2\right)}. \tag{26}$$

After expanding the cosine which appears in equation (25) and after noticing that $J_0(u_0)$ and $\mathrm{i}^n J_n(u_0)$ are always real, the expression for the symmetric kernel in the undamped case finally reads

$$K_0(\lambda) = \Delta^2 \mathrm{e}^Y \int_0^\infty \mathrm{d}\tau \mathrm{e}^{-\lambda\tau} \left[J_0(u_0) + 2\sum_{n=1}^{+\infty} (-\mathrm{i})^n J_n(u_0) \cos\left(n\Omega\tau\right) \cosh\left(n\frac{\hbar\beta\Omega}{2} \right) \right]. \tag{27}$$

In order to enhance the readability of the kernel, we define the dressed frequencies

$$\Delta_{n_{(c)}} \equiv \Delta \mathrm{e}^{Y/2} \sqrt{(2 - \delta_{n,0})\,(-\mathrm{i})^n J_n(u_0) \cosh\left(n\frac{\hbar\beta\Omega}{2} \right)}, \tag{28}$$

such that we can rewrite equation (27) in the very compact form

$$K_0(\lambda) = \sum_{n=0}^{+\infty} \Delta^2_{n_{(c)}} \int_0^\infty \mathrm{d}\tau \mathrm{e}^{-\lambda\tau} \cos\left(n\Omega\tau\right). \tag{29}$$

The population difference $P_0(\lambda)$ in the undamped case becomes

$$P_0(\lambda) = \frac{1}{\lambda + K_0(\lambda)} \tag{30}$$

$$= \frac{1}{\lambda\left[1 + \sum_{n=0}^{+\infty} \Delta^2_{n_{(c)}} \frac{1}{\lambda^2 + n^2\Omega^2}\right]} \tag{31}$$

$$= \frac{\lambda^2 \prod_{n=1}^{\infty} (\lambda^2 + n^2\Omega^2)}{\lambda\left[\prod_{n=0}^{\infty} (\lambda^2 + n^2\Omega^2) + \sum_{m=0}^{+\infty} \Delta^2_{m_{(c)}} \prod_{\substack{n=0 \\ n\neq m}}^{+\infty} (\lambda^2 + n^2\Omega^2)\right]}, \tag{32}$$

and it is clear that the pole in $\lambda = 0$ is not a physical one, since $P_0(\lambda = 0)$ vanishes. This means that the dissipation-free ($\kappa = 0$) pole equation reads

$$\lambda_\mathrm{p} + K_0(\lambda_\mathrm{p}) = 0 \quad \rightarrow \quad \prod_{n=0}^{\infty} (\lambda_\mathrm{p}^2 + n^2\Omega^2) + \sum_{m=0}^{+\infty} \Delta^2_{m_{(c)}} \prod_{\substack{n=0 \\ n\neq m}}^{+\infty} (\lambda_\mathrm{p}^2 + n^2\Omega^2) = 0. \tag{33}$$

Notice that being the pole equation of infinite order in λ_p^2, equation (33) implies that an *infinite* set of frequencies enters the dynamics, which can be attributed to the entanglement of the TSS with the HO. Their temperature dependence, included in the dressed frequencies $\Delta_{n(c)}$, reflects in a nontrivial way the initial thermal state of the HO. We shall show below that in some parameter regimes only few of these frequencies dominate the dynamics.

4.2. The weak-damping population difference $P(t)$

The weak-damping kernel $K_{\rm WDA}(\lambda)$ is obtained from equation (13) by retaining only terms up to first order in the linearized in κ bath correlation functions Q_1' and Q_1''. It reads

$$K_{\rm WDA}(\lambda) = \Delta^2 \int_0^\infty {\rm d}\tau {\rm e}^{-\lambda\tau}\, {\rm e}^{-Q_0'(\tau)} \left\{ \cos\left(Q_0''(\tau)\right) \left[1 - Q_1'(\tau)\right] - \sin\left(Q_0''(\tau)\right) Q_1''(\tau) \right\}. \tag{34}$$

The WDA kernel will be used in equation (11) to solve the pole equation and finally obtain $P_{\rm WDA}(t)$. Consistent with the previous prescription $\kappa \ll 1$, we can expand the solutions λ^* of the pole equation around the solutions $\lambda_{\rm p}$ of the non-interacting pole equation up to first-order in κ. In other terms

$$\lambda^* = \lambda_{\rm p} - \kappa\gamma_{\rm p} + {\rm i}\kappa\varphi, \tag{35}$$

where $\lambda_{\rm p}$ satisfies the undamped pole equation (33). By inserting equations (15) and (35) in (34), one finds the following expressions for the WDA kernel evaluated at the poles:

$$\begin{aligned} K_{\rm WDA}(\lambda^*) = \Delta^2 \int_0^\infty {\rm d}\tau {\rm e}^{-\lambda_{\rm p}\tau}\, {\rm e}^{-Q_0'(\tau)} \\ \times \left\{ \cos\left(Q_0''(\tau)\right) \left[1 + \kappa\gamma_p\tau - {\rm i}\kappa\varphi\tau - Q_1'(\tau)\right] - \sin\left(Q_0''(\tau)\right) Q_1''(\tau) \right\} + \mathcal{O}[\kappa^2]. \end{aligned} \tag{36}$$

According to equation (36), the pole equation (11) now reads

$$\begin{aligned} -\kappa\gamma_{\rm p} + {\rm i}\kappa\varphi + \Delta^2 \int_0^\infty {\rm d}\tau {\rm e}^{-\lambda_{\rm p}\tau}\, {\rm e}^{-Q_0'(\tau)} \\ \times \left\{ \cos\left(Q_0''(\tau)\right) \left[\kappa\gamma_{\rm p}\tau - {\rm i}\kappa\varphi\tau - Q_1'(\tau)\right] - \sin\left(Q_0''(\tau)\right) Q_1''(\tau) \right\} = 0, \end{aligned} \tag{37}$$

where we used the pole equation for the undamped case (19). After isolating the real and the imaginary terms from the above equation[5], we find

$$\begin{aligned} -\kappa\gamma_{\rm p} \left[1 - \Delta^2 \int_0^\infty {\rm d}\tau {\rm e}^{-\lambda_{\rm p}\tau}\, {\rm e}^{-Q_0'(\tau)} \cos\left(Q_0''(\tau)\right) \tau \right] \\ = \Delta^2 \int_0^\infty {\rm d}\tau {\rm e}^{-\lambda_{\rm p}\tau}\, {\rm e}^{-Q_0'(\tau)} \left[\cos\left(Q_0''(\tau)\right) Q_1'(\tau) + \sin\left(Q_0''(\tau)\right) Q_1''(\tau) \right], \end{aligned} \tag{38a}$$

$${\rm i}\kappa\varphi \left[1 - \Delta^2 \int_0^\infty {\rm d}\tau {\rm e}^{-\lambda_{\rm p}\tau}\, {\rm e}^{-Q_0'(\tau)} \cos\left(Q_0''(\tau)\right) \tau \right] = 0. \tag{38b}$$

if the term between brackets is different from zero, one easily gets $\varphi = 0$ and, after some rearrangements,

$$\gamma_{\rm p} = -\frac{\Delta^2}{\kappa} \frac{\int_0^\infty {\rm d}\tau {\rm e}^{-\lambda_{\rm p}\tau}\, {\rm e}^{-Q_0'(\tau)} \left[\cos\left(Q_0''(\tau)\right) Q_1'(\tau) + \sin\left(Q_0''(\tau)\right) Q_1''(\tau) \right]}{\left[1 + \frac{\partial}{\partial\lambda} K_0(\lambda) \right]\Big|_{\lambda=\lambda_{\rm p}}}. \tag{39}$$

[5] Note that the Laplace transform of an odd function of τ is even in λ and vice versa. In this case, the integrand is odd in τ, thus the corresponding Laplace transform is even in λ. For pure-imaginary values of λ, the result of the integral is real.

Once we have obtained the expression for the decay rates γ_p corresponding to each pole λ_p, we have all the ingredients to get the population difference $P(t)$ with the help of the residue theorem. In fact,

$$P(t) \equiv \sum_{\text{Res}} e^{\lambda t} P(\lambda) = \sum_{\text{Res}} e^{\lambda t} \frac{1}{\lambda + K_{\text{WDA}}(\lambda)}$$
$$= \sum_{\lambda_p} e^{\lambda_p t} e^{-\kappa \gamma_p(\lambda_p) t} \lim_{\lambda \to \lambda_p - \kappa\gamma_p} [\lambda - (\lambda_p - \kappa\gamma_p)] \frac{1}{\lambda + K_{\text{WDA}}(\lambda)} \tag{40}$$

holds, as follows from equation (36).

4.3. Series expression for the weakly-damped symmetric kernel and decay rate

In this subsection, we show how to obtain a compact analytical form for the kernel $K_{\text{WDA}}(\lambda)$ and the decay rate γ_p equations (34) and (39), respectively. To this end let us start from the kernel $K_{\text{WDA}}(\lambda)$, the generalization to the decay rate being straightforward. As in the undamped case, in equation (34) we replace $\cos(Q_0''(\tau))$ with $\text{Re}\{\exp(iQ_0''(\tau))\}$ and $\sin(Q_0''(\tau))$ with $\text{Im}\{\exp(iQ_0''(\tau))\}$. Analogously to the procedure followed for the undamped kernel (29), by using the Jacobi–Anger expansion (21) we obtain

$$K_{\text{WDA}}(\lambda) = \sum_{n=0}^{+\infty} \int_0^{\infty} d\tau e^{-\lambda\tau} \left\{ \Delta_{n_{(c)}}^2 \cos(n\Omega\tau) \left[1 - Q_1'(\tau)\right] + \Delta_{n_{(s)}}^2 \sin(n\Omega\tau) Q_1''(\tau) \right\}, \tag{41}$$

where the dressed tunneling elements $\Delta_{n_{(c)}}$ have been already defined in equation (28a) and

$$\Delta_{n_{(s)}} \equiv \Delta e^{Y/2} \sqrt{(2 - \delta_{n,0})\,(-i)^n J_n(u_0) \sinh\left(n\frac{\beta\Omega}{2}\right)}. \tag{42}$$

The expression for $P(\lambda)$ follows from (41) (see the discussion in the section 4.5 below). Along similar lines, the decay rate γ_p, cf equation (39), may also be written as

$$\gamma_p = \frac{1}{\kappa} \frac{\sum_{n=0}^{+\infty} \int_0^{\infty} d\tau e^{-\lambda_p \tau} \left[\Delta_{n_{(c)}}^2 \cos(n\Omega\tau)\, Q_1'(\tau) + \Delta_{n_{(s)}}^2 \sin(n\Omega\tau)\, Q_1''(\tau) \right]}{\sum_{n=0}^{+\infty} \Delta_{n_{(c)}}^2 \frac{2\lambda_p^2}{(\lambda_p^2 + n^2\Omega^2)^2}}. \tag{43}$$

4.4. The case $n = 0, n = 1$

In the following, we investigate the regime of temperatures $\beta\hbar\Omega/2 \gtrsim 1$, and of coupling $\Gamma < g \ll \Omega$, such that the quantity u_0 entering the argument of the Bessel functions is smaller than one. Then, because the amplitudes Δ_n^2 in (41) depend on Bessel functions $J_n(x)$, which roughly behave as x^n as soon as the argument becomes small, we can restrict our analysis to the terms $n = 0, n = 1$ in equations (41) and (43). We identify here Δ_0 with $\Delta_{0_{(c)}}$ and Δ_1 with $\Delta_{1_{(c)}}$ for the sake of clarity, which in the considered regime are approximately given by

$$\Delta_0^2 = \Delta^2 e^Y J_0(u_0) \approx \Delta^2 e^Y = \Delta^2 e^{-(2g/\Omega)^2}, \tag{44}$$

and

$$\Delta_1^2 = \Delta^2 e^Y (-2i) J_1(u_0) \cosh\left(\frac{\hbar\beta\Omega}{2}\right) \approx \Delta_0^2 (2g/\Omega)^2. \tag{45}$$

The undamped pole equation (33) becomes

$$(\lambda_p^2+\Omega^2)(\lambda_p^2+\Delta_0^2)+\lambda_p^2\Delta_1^2=0, \tag{46}$$

yielding

$$\lambda_p^2=-\frac{\Delta_0^2+\Delta_1^2+\Omega^2}{2}\pm\sqrt{\left(\frac{\Delta_0^2-\Omega^2}{2}\right)^2+\frac{\Delta_1^2}{2}\left(\Delta_0^2+\frac{\Delta_1^2}{2}+\Omega^2\right)}\equiv\lambda_\pm^2. \tag{47}$$

As becomes clear from the definition of the dressed frequencies Δ_0^2, Δ_1^2 these quantities, and in turn the frequencies $-\Omega_\pm^2\equiv\lambda_\pm^2$ depend on oscillator frequency Ω, TSS splitting Δ and coupling strength g.

We notice that only terms quadratic in λ_p appear in the formal expression of the decay rate (cf equation (B.1)). Hence, it is enough to express the poles as in equation (47). Given the poles in the undamped case, we can substitute each of them in equation (43) for γ_p with sum restricted to $n=0$, $n=1$. We will refer to them as $\gamma_\pm=\gamma(\lambda_\pm)$, the explicit form of the decay rate being given in appendix B.

4.5. Analytical expression for $P(t)$

In order to obtain the analytical expression for $P(t)$ in the symmetric case, let us start again from equation (40). By summing up all residues contributions, we end up with

$$P(t)=\mathrm{e}^{-\kappa\gamma_- t}\frac{\lambda_-^2+\Omega^2}{\lambda_-^2-\lambda_+^2}[\cos(\Omega_- t)-\frac{\kappa\gamma_-}{\Omega_-}\sin(\Omega_- t)]+\mathrm{e}^{-\kappa\gamma_+ t}\frac{\lambda_+^2+\Omega^2}{\lambda_+^2-\lambda_-^2}[\cos(\Omega_+ t)-\frac{\kappa\gamma_+}{\Omega_+}\sin(\Omega_+ t)], \tag{48}$$

where $\Omega_\pm\equiv-\mathrm{i}\lambda_\pm$, as follows from equation (47). Notice that the expression for $P(t)$ is invariant upon exchanging the frequencies $\Omega_-\to\Omega_+$. The analytical formula equation (48) for $P(t)$ is compared in figure 4 with the outcomes of a numerical solution of the NIBA GME and with the conventional weak-coupling approximation (WCA). The latter is obtained by performing an expansion of the NIBA kernel to first-order in the coupling strength α [2]. The analytical form for the probability difference reads in the WCA case

$$P(t)=\left\{\cos\Delta t+\frac{\gamma_\varphi}{\Delta}\sin\Delta t\right\}\mathrm{e}^{-\gamma_\varphi t}, \tag{49}$$

where $\gamma_\varphi=(\pi/4)S(\Delta)$ is the dephasing rate. Moreover, $S(\omega)\equiv G_{\mathrm{eff}}(\omega)\coth(\hbar\omega/2k_\mathrm{B}T)$ is a spectral contribution which represents emission and absorption of a single phonon. The choice of parameters in figures 4 and 5 is the same as in figure 1 and as in [23], under the resonance condition $\Omega=\Delta$. One can notice a very good agreement between NIBA and analytical WDA, whereas equation (49) completely fails in describing the oscillatory behaviour of $P(t)$. In figure 5 the corresponding Fourier transform of the probability difference is shown. There, one can see the missing oscillation frequency of the conventional WCA given by equation (49) and the excellent agreement between the numerical NIBA and our analytical solution WDA. The WCA in fact is not applicable since the bath is not short-time correlated when $g>\Gamma$ [23]. Notice also that in the resonant case the WCA overestimates dephasing because there are coherent exchange processes between the TSS and the resonant HO which cannot be captured by such a weak-coupling scheme.

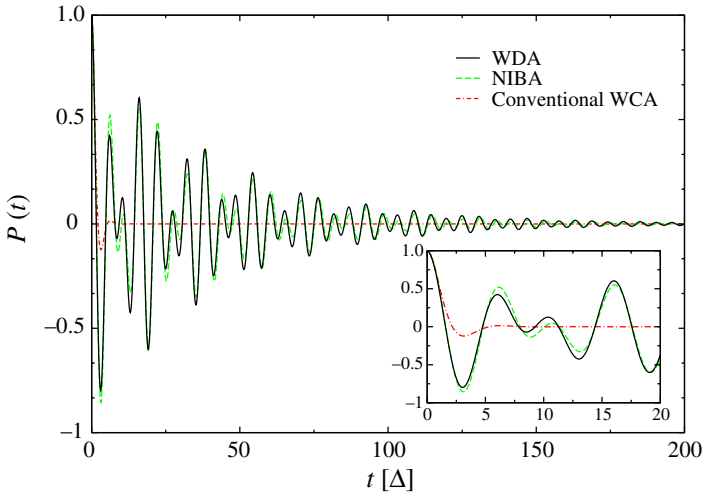

Figure 4. Time evolution of $P(t)$ within the NIBA as well as the analytical WDA. The parameters are as in figure 1, namely $\Omega = 1$, $\Gamma = 0.097$, $\alpha = 4 \times 10^{-3}$ ($g = 0.18$), $T = 0.1$ (in units of Δ). Notice the perfect agreement between the numerical NIBA and the analytical WDA. A perturbative approach in $G_{\mathrm{eff}}(\omega)$, denoted here as 'conventional WCA' (see (49)), completely fails to account for the two main oscillation frequencies. In the inset the short-time dynamics is magnified.

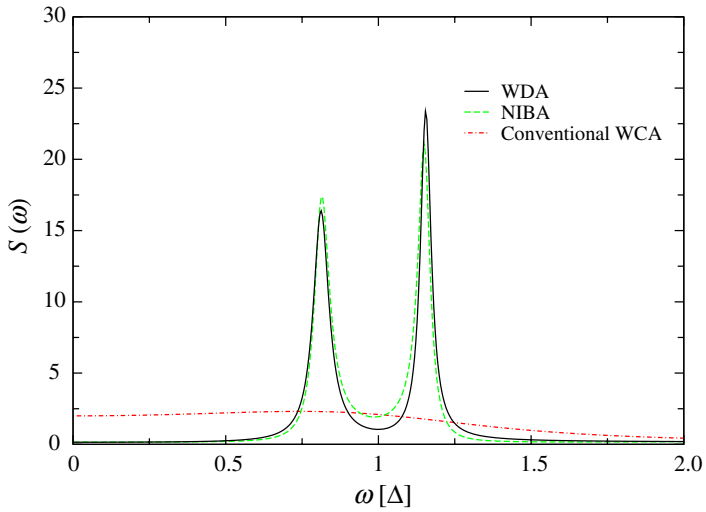

Figure 5. Spectral function of $P(t)$, corresponding to the same regime as in the previous case. One clearly sees that the Fourier transforms of NIBA and WDA exhibit a double peak structure. In contrast, the WCA predicts a single broadened oscillation peak.

Equation (47) together with equations (44) and (45) enable us to estimate the oscillation frequency. Specifically, let us observe that the resonance condition is $\Omega = \Delta_0$ rather than $\Omega = \Delta$, though the two frequencies Δ and Δ_0 are very close in the chosen regime of parameters.

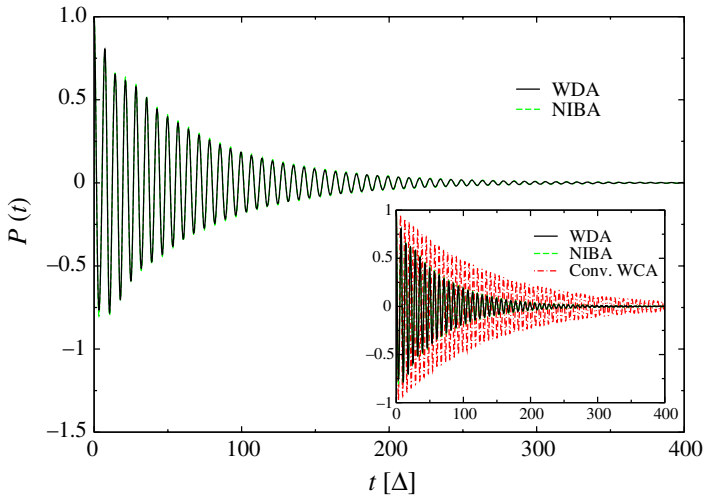

Figure 6. Time evolution of $P(t)$ at finite detuning within the NIBA and the analytical WDA. The parameters are as in figure 2, namely $\Omega = 1.5$, $\Gamma = 0.145$, $T = 0.1$ (in units of Δ), and $\alpha = 5 \times 10^{-3}$ corresponding to $g = 0.3$. Again, the agreement between the numerical NIBA and the analytical WDA is striking. Inset: the conventional WCA (49) also in this case, as expected, fails in describing the correct dynamics.

For $\Omega = \Delta_0$ and with $\Delta_1 \ll \Delta_0$, we obtain to lowest order in Δ_1 the expression

$$\Omega_{\pm} \approx \Omega \left(1 \mp \frac{\Delta_1}{2\Omega}\right), \tag{50}$$

such that $\Omega_- - \Omega_+ = 2\,g$ as in the simple Jaynes–Cummings model.

Finally, in figure 6 we show a comparison among the WDA and the NIBA in the presence of finite detuning $\delta \equiv |\Delta - \Omega| = 0.5\Delta$ for a higher coupling strength between qubit and HO ($g = 0.3\Delta$), keeping the coupling between detector and environment constant. Also in this case, the WDA fully agrees with the numerical solution of the NIBA. From (47) we find, neglecting terms of order Δ_1^4, and assuming e.g. $\Omega > \Delta_0$

$$\Omega_- \approx \Omega \left(1 + \frac{\Delta_1^2}{2(\Omega^2 - \Delta_0^2)}\right), \tag{51}$$

$$\Omega_+ \approx \Delta_0 \left(1 - \frac{\Delta_1^2}{2(\Omega^2 - \Delta_0^2)}\right), \tag{52}$$

yielding $\Omega_- - \Omega_+ = \delta(1 + \frac{g^2}{\delta^2}\frac{2\Delta_0^2}{\Omega^2})$. The frequency Ω_- is nicely interpreted as the Stark-shifted qubit frequency due to the coupling with the harmonic mode; the frequency Ω_+ accounts for processes involving absorption of a single oscillator quantum whose amplitude, however, is strongly suppressed, see figure 7 which shows the Fourier transform of $P(t)$. In the inset one can also notice the disagreement of the WDA predictions with the conventional WCA, characterized by a single oscillation frequency at $\omega = \Delta$.

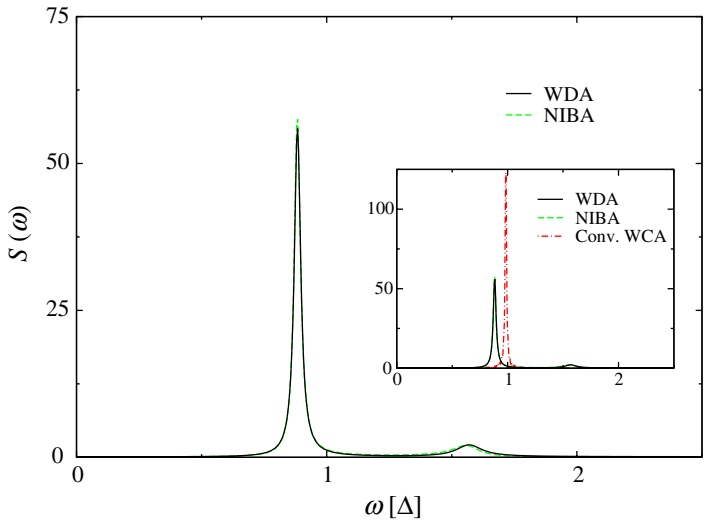

Figure 7. Spectral function of $P(t)$ for the NIBA and the analytical WDA (same parameters as in figure 6). The oscillation frequencies of WDA and NIBA coincide, whereas in the inset one can at first glance see the occurrence of a single peak only in the Fourier transform of the conventional WCA.

5. Conclusions

In conclusion, we discussed the dynamics of a symmetric TSS interacting with an effective structured environment described by a spectral density $G_{\rm eff}$. This models e.g. a qubit interacting with a dissipative detector [6, 7], or a TSS interacting with a cavity mode [12, 13]. Focussing on the regime of small coupling κ between the oscillator and an Ohmic bath, i.e. of large Q factors of the damped harmonic mode, we derived a GME for the TSS occupation probabilities within a novel *weak damping approximation*. In contrast to 'conventional' weak-coupling approaches [2], perturbative in $G_{\rm eff}$, the WDA is able to reproduce multiple oscillation frequencies in the TSS dynamics resulting from the entanglement with the oscillator. The starting point of our analysis is the NIBA, which for a symmetric spin–boson model is valid over the *whole* range of parameters. The NIBA is perturbative in the TSS tunneling frequency, but nonperturbative in the bath effective spectral density $G_{\rm eff}$. The WDA approach is then based on an expansion of $G_{\rm eff}$ up to first-order in the coupling κ. The zeroth order term describes the effects of the entanglement between the TSS and the undamped thermalized mode; the linear term is responsible for the dephasing. As a result of the entanglement with the damped mode, the TSS is generally characterized by a multiple set of frequencies, as detailed in section 4. However, for small enough temperatures (i.e. $k_{\rm B}T \lesssim \hbar\Omega$) and moderate TSS-harmonic mode coupling $\Gamma < g \ll \Omega$ only two frequencies dominate, whose values, as well as those of the associated dephasing rates, are determined analytically. In the resonant regime the two frequencies are those expected from a simple Jaynes–Cummings model, apart from the fact that the resonance condition now reads $\Omega = \Delta_0$, where Δ_0 is the *dressed* TSS frequency in equation (44). At finite detuning the one that is associated with a Stark-shifted TSS frequency splitting dominates, see equation (52). The less dominant frequency occurs due to processes related to the absorption of a single oscillator quantum. The agreement of our

analytical solution for the TSS occupation probability, valid at *arbitrary* detuning $|\Delta - \Omega| \neq 0$, with the numerical outcomes of the NIBA is striking.

Due to the generality of the model, we expect our results to be of interest in many experimental applications.

Acknowledgments

We acknowledge financial support under the DFG program SFB631, EU-EuroSQIP (IST-3-015708-IP) and MIUR-PRIN2005 (2005022977).

Appendix A. Bessel function expansion of the NIBA kernels

Here we are interested in finding a series expression for the WDA kernel which contains Bessel functions. We start from equation (34), which we rewrite for clarity:

$$K(\lambda) = \Delta^2 \int_0^\infty \mathrm{d}\tau \mathrm{e}^{-\lambda\tau}\, \mathrm{e}^{-Q_0'(\tau)} \left\{ \cos\left(Q_0''(\tau)\right) \left[1 - Q_1'(\tau)\right] - \sin\left(Q_0''(\tau)\right) Q_1''(\tau) \right\}. \tag{A.1}$$

Let us examine, to fix the ideas, the term $\exp\{-Q_0'(\tau)\}\cos(Q''_0(\tau))$:

$$\mathrm{e}^{-Q_0'(\tau)} \cos\left(Q_0''(\tau)\right) \equiv \mathrm{e}^{Y} \mathrm{Re}\left\{ \mathrm{e}^{-Y\cos\Omega\tau} \mathrm{e}^{+\mathrm{i}W\sin\Omega\tau} \right\} \tag{A.2}$$

$$= \mathrm{e}^{Y} \mathrm{Re}\left\{ \mathrm{e}^{\mathrm{i}[\mathrm{i}Y\cos\Omega\tau + W\sin\Omega\tau]} \right\} \tag{A.3}$$

$$= \mathrm{e}^{Y} \mathrm{Re}\left\{ \mathrm{e}^{\mathrm{i}\sqrt{W^2-Y^2}\left[\frac{\mathrm{i}Y}{\sqrt{W^2-Y^2}}\cos\Omega\tau + \frac{W}{\sqrt{W^2-Y^2}}\sin\Omega\tau\right]} \right\}. \tag{A.4}$$

It could be now convenient to interpret

$$\begin{cases} \cos x \equiv \dfrac{\mathrm{i}Y}{\sqrt{W^2 - Y^2}} = +\dfrac{Y}{\sqrt{Y^2 - W^2}}, & (A.5a) \\ \sin x \equiv \dfrac{-W}{\sqrt{W^2 - Y^2}} = +\dfrac{\mathrm{i}W}{\sqrt{Y^2 - W^2}}, & (A.5b) \end{cases}$$

so that the exponent can be rewritten as

$$\mathrm{e}^{-Q_0'(\tau)} \cos\left(Q_0''(\tau)\right) = \mathrm{e}^{Y} \mathrm{Re}\left\{ \mathrm{e}^{\mathrm{i}\sqrt{W^2-Y^2}} \cos\left(\Omega\tau + x\right) \right\}. \tag{A.6}$$

At this point, we can use the Jacobi–Anger expansion (21) to expand the exponent in series of Bessel functions. We finally obtain

$$K(\lambda) = \Delta^2 \mathrm{e}^{Y} \int_0^\infty \mathrm{d}\tau \mathrm{e}^{-\lambda\tau} \left\{ \left[J_0(u_0) + 2\sum_{n=1}^{+\infty} (-\mathrm{i})^n J_n(u_0) \cos\left(n\Omega\tau\right) \cosh\left(n\frac{\beta\hbar\Omega}{2}\right) \right] \right.$$
$$\left. \times \left[1 - Q_1'(\tau)\right] + 2\sum_{n=1}^{+\infty} (-\mathrm{i})^n J_n(u_0) \sin\left(n\Omega\tau\right) \sinh\left(n\frac{\beta\hbar\Omega}{2}\right) Q_1''(\tau) \right\}, \tag{A.7}$$

which coincides with equation (41), once we introduce the amplitudes $\Delta_{n(c)}$, $\Delta_{n(s)}$. Here, u_0 is given by

$$u_0 \equiv \sqrt{W^2 - Y^2} = \mathrm{i}\sqrt{Y^2 - W^2} = \mathrm{i}\frac{4g^2}{\Omega^2} \frac{1}{\sinh\left(\beta\hbar\Omega/2\right)}, \tag{A.8}$$

since $Y \equiv -W\coth(\beta\hbar\Omega/2)$ (note that $W > 0$ and hence $Y < 0$). Notice that the argument of the Bessel functions is small whenever $\beta\hbar\Omega/2 \gtrsim 1$ and $g \lesssim \Omega$.

We would like now to obtain the exact value of x, which is easily performed. Let us start from equation (A.5) and let us rewrite the tangent as

$$\tan x = \frac{+\mathrm{i}W}{Y} = -\mathrm{i}\tanh\left(\frac{\beta\hbar\Omega}{2}\right) = \tan\left(-\mathrm{i}\frac{\beta\hbar\Omega}{2}\right). \tag{A.9}$$

We assume x to be complex, therefore we write it as $x = a + \mathrm{i}b$. In general, it holds that

$$\cos(a + \mathrm{i}b) = \cos a \cosh b - \mathrm{i}\sin a \sinh b, \tag{A.10}$$

$$\sin(a + \mathrm{i}b) = \sin a \cosh b + \mathrm{i}\cos a \sinh b. \tag{A.11}$$

From (A.10), in order to have $\cos(a + \mathrm{i}b) = +Y/\sqrt{Y^2 - W^2}$, namely a real number, it must be that

$$a = n\pi. \tag{A.12}$$

From equations (A.10) and (A.11), we can write the tangent as

$$\tan(a + \mathrm{i}b) = \frac{\tan a + \mathrm{i}\tanh b}{1 - \mathrm{i}\tan a \tanh b} \xrightarrow[a=n\pi]{} +\mathrm{i}\tanh b \equiv +\mathrm{i}\frac{W}{Y}, \tag{A.13}$$

as we get by calculating the tangent from equation (A.5). Hence,

$$\tanh b = \frac{W}{Y}. \tag{A.14}$$

We can eventually write x as

$$x \equiv a + \mathrm{i}b = n\pi + \mathrm{i}\,\mathrm{arc}\tanh\frac{W}{Y} = n\pi - \mathrm{i}\frac{\beta\hbar\Omega}{2}. \tag{A.15}$$

In order to decide whether to assume $n = 0$ or $n = 1$, one must look at the cosine or sine:

$$\cos x \xrightarrow[a=n\pi]{\text{equation (A.10)}} (-1)^n \frac{1}{\sqrt{1 - \tanh^2 b}} = (-1)^n \frac{1}{\sqrt{1 - \frac{W^2}{Y^2}}} = (-1)^n \frac{|Y|}{\sqrt{Y^2 - W^2}} \tag{A.16}$$

$$\equiv \frac{+Y}{\sqrt{Y^2 - W^2}} < 0, \qquad \Longmapsto n = 1 \tag{A.17}$$

or, equivalently,

$$\sin x \xrightarrow[a=n\pi]{\text{equation (A.11)}} \mathrm{i}(-1)^n \frac{\tanh b}{\sqrt{1 - \tanh^2 b}} = \mathrm{i}(-1)^n \frac{W/Y}{\sqrt{1 - (W^2/Y^2)}} \tag{A.18}$$

$$= \mathrm{i}(-1)^n \frac{(W/Y)|Y|}{\sqrt{Y^2 - W^2}} = -\mathrm{i}(-1)^n \frac{W}{\sqrt{Y^2 - W^2}} \equiv \frac{+\mathrm{i}W}{\sqrt{Y^2 - W^2}}, \qquad \Longmapsto n = 1. \tag{A.19}$$

Appendix B. Explicit form for the decay rate γ_{p}

In this appendix, we wish to give the analytical result for the decay rate $\gamma_{\mathrm{p}}(\lambda_{\mathrm{p}})$ as function of the solution λ_{p} of the undamped pole equation (46):

$$\gamma_{\mathrm{p}}(\lambda_{\mathrm{p}}) = \frac{1}{\kappa}\frac{1}{2\lambda_{\mathrm{p}}^2\left[(\lambda_{\mathrm{p}}^2+\Omega^2)^2+\Delta_{1_{(c)}}^2\Omega^2\right]}\Bigg[\lambda_{\mathrm{p}}^2\left(p+q\Delta_{1_{(c)}}^2+t\Delta_{1_{(s)}}^2+u\Delta_{1_{(c)}}^2\Delta_{1_{(s)}}^2+r\Delta_{1_{(c)}}^4\right)$$
$$+\Omega^2\left(s+w\Delta_{1_{(c)}}^2+t\Delta_{1_{(s)}}^2\right)+\lambda_{\mathrm{p}}^2\left(\Delta_{1_{(c)}}^2 g(\lambda_{\mathrm{p}})+\Delta_{1_{(s)}}^2 h(\lambda_{\mathrm{p}})\right)\Bigg], \tag{B.1}$$

with

$$p \equiv (2A-B)\Omega^2\Delta_0^2+(B-D)\Delta_0^4, \tag{B.2}$$

$$q \equiv \Delta_0^2\left(\frac{A}{2}+2B-D\right)+\Omega^2\left(2B-\frac{A}{2}\right), \tag{B.3}$$

$$t \equiv -\frac{V\Omega}{4}(\Omega^2+3\Delta_0^2), \tag{B.4}$$

$$u \equiv -3\frac{V\Omega}{4}, \tag{B.5}$$

$$r \equiv \frac{A}{2}+B, \tag{B.6}$$

$$s \equiv -\Omega^2\Delta_0^2 B+\Delta_0^4(B-D), \tag{B.7}$$

$$w \equiv \Delta_0^2\left(\frac{A}{2}+B\right)-\Omega^2\frac{A}{2} \tag{B.8}$$

and

$$g(\lambda_{\mathrm{p}}) \equiv \frac{(\lambda_{\mathrm{p}}^2+\Omega^2)^2}{\lambda_{\mathrm{p}}^2+4\Omega^2}\left(C\Omega+\frac{A}{2}\frac{\lambda_{\mathrm{p}}^2-4\Omega^2}{\lambda_{\mathrm{p}}^2+4\Omega^2}\right), \tag{B.9}$$

$$h(\lambda_{\mathrm{p}}) \equiv \frac{(\lambda_{\mathrm{p}}^2+\Omega^2)^2}{\lambda_{\mathrm{p}}^2+4\Omega^2}\frac{V\Omega}{4}\frac{3\lambda_{\mathrm{p}}^2+20\Omega^2}{\lambda_{\mathrm{p}}^2+4\Omega^2}. \tag{B.10}$$

As already seen, the physical poles are $\lambda^2 = -\lambda_{1,2}^2 \equiv \lambda_{\pm}^2$. Correspondingly, the decay rates $\gamma_{\pm} = \gamma(\lambda_{\pm})$ follow according to equation (B.1).

References

[1] Leggett A J *et al* 1987 *Rev. Mod. Phys.* **59** 1
[2] Weiss U 1999 *Quantum Dissipative Systems* 2nd edn (Singapore: World Scientific)
[3] Grifoni M and Hänggi P 1998 *Phys. Rep.* **304** 229
[4] Makhlin Y, Schön G and Shnirman A 2001 *Rev. Mod. Phys.* **73** 357
[5] van der Wal C *et al* 2000 *Science* **290** 773
[6] Chiorescu I *et al* 2003 *Science* **299** 1869
[7] Chiorescu I *et al* 2004 *Nature* **431** 159

[8] Tian L, Lloyd S and Orlando T P 2002 *Phys. Rev.* B **65** 144516
[9] van der Wal C H, Wilhelm F K, Harmans C J P M and Mooij J E 2003 *Eur. Phys. J.* B **31** 111
[10] Garg A, Onuchic J N and Ambegaokar V 1985 *J. Chem. Phys.* **83** 4491
[11] Haroche S 2001 *Rev. Mod. Phys.* **73** 565
[12] Wallraff A *et al* 2004 *Nature* **431** 162
[13] Schuster D *et al* 2007 *Nature* **445** 515
[14] Badolato A *et al* 2005 *Science* **308** 1158
[15] Blencowe M 2004 *Phys. Rep.* **395** 159
[16] Schleich W P 2001 *Quantum Optics in Phase Space* (New York: Wiley)
[17] Blais A *et al* 2004 *Phys. Rev.* A **69** 062320
[18] Sarovar M *et al* 2007 *Phys. Rev.* A **72** 062327
[19] Gambetta J *et al* 2006 *Phys. Rev.* A **74** 042318
[20] Serban I, Solano E and Wilhelm F K 2006 *Preprint* cond-mat/0606734v4
Serban I, Solano E and Wilhelm F K 2007 *Preprint* cond-mat/0703005v1
[21] Clerk A A and Utami D W 2007 *Phys. Rev.* A **75** 042302
[22] Jaynes E T and Cummings F W 1963 *IEEE Proc.* **51** 90
[23] Thorwart M, Paladino E and Grifoni M 2004 *Chem. Phys.* **296** 333
[24] Goorden M C and Wilhelm F K 2003 *Phys. Rev.* B **68** 012508
[25] Goorden M C, Thorwart M and Grifoni M 2004 *Phys. Rev. Lett.* **93** 267005
Goorden M C, Thorwart M and Grifoni M 2005 *Eur. Phys. J.* B **45** 405
[26] Thorwart M *et al* 2000 *J. Mod. Opt.* **47** 2905
[27] Smirnov A Yu 2003 *Phys. Rev.* B **67** 155104
[28] Wilhelm F K, Kleff S and von Delft J 2004 *Chem. Phys.* **296** 345
[29] Kleff S, Kerhein S and von Delft J 2004 *Phys. Rev.* B **70** 014516
[30] Huang P and Zeng H 2007 *Preprint* 0707.0725
[31] Gradshteyn I S and Ryzhik I M 1965 *Tables of Integrals, Series and Products* (London: Academic)